ISSN: 2321-7782 (Online)
Volume 2, Issue 4, April 2014
International Journal of Advance Research in Computer Science and Management Studies
Research Article / Paper / Case Study
Available online at: www.ijarcsms.com

Lung Nodules Detection by Computer Aided Diagnosis (CAD) Using Image Processing

V.Sampath Kumar[1]
PG Scholar, Embedded Systems
CMS College of Engineering
Namakkal (Dt), Tamilnadu - India

P.Sathees Kumar[2]
Assistant Professor, ECE Department
CMS College of Engineering
Namakkal (Dt), Tamilnadu - India

Abstract: ***The detection of the lung nodules can be found out by introducing Computer Aided Diagnosis (CAD) scheme. The Purpose is to develop a CADe scheme with improved sensitivity and specificity to detect the lung nodules by Virtual Dual Energy (VDE) method. The ribs and clavicles induced lung nodules can be specified out by a technique called Feed Forward Neural Network technique. In this work a CADe scheme for detection of pulmonary nodules by use of the Grey level co occurrence matrix and by Nodule Enhancement to improve the sensitivity for nodules overlapping ribs and clavicles and to reduce FPs caused by these structures. Finally the total number of nodules that are affected in the lung region can be found out by using the FFNN technique. By comparing the nodules and non-nodules images, we can get the improved sensitivity. The overall sensitivity and specificity has been improved by using the VDE technology. Therefore, by use of this technology, the sensitivity has been increased to 87% from78.6%.***

Keywords: Chest Radiography (CXR), Computer Aided Diagnosis (CAD), Feed Forward Neural Network (FFNN), Multiple Training Artificial Neural Network (MTANN), Virtual Dual Energy (VDE).

I. INTRODUCTION

Early detection and treatment of lung cancer are crucially important for improvement of the patient survival rate. The patient survival rate can be improved greatly if the carcinoma is found and removed at this early stage. Although chest radiographs are the most widely used modality for screening of lung cancers, studies show that radiologists could fail to detect pulmonary nodules in chest radiographs in up to 30% of actually abnormal cases.

To assist radiologists in the diagnosis of lung diseases, therefore, we are developing a computer-aided diagnosis (CAD) scheme for the detection of pulmonary nodules in digital chest radio-graphs. The output from the computer would be used to alert radiologists to potential nodule locations, and the final diagnostic decision would then be made by the radiologists.

A major obstacle in obtaining high performance for a computerized detection scheme is related to the problem of how to reduce the false-positive detection rate, because although several computerized methods for automated detection of nodules have been investigated many of these methods suffer from a large number of false positives. The number of false positives would have to be increased to a range of five to more than ten per image for a clinically accept-able level of sensitivity to be achieved.

II. MATERIALS AND METHODS

A. MTANN SCHEME FOR THE LUNG NODULE DETECTION

To address the issue of the availability of dual-energy systems, Suzuki *et al*. developed an image-processing technique called virtual dual energy (VDE) radiography for suppressing ribs and clavicles in CXRs by means of MTANN. The dual-energy images were used as the teaching images for training of the multi resolution MTANN. The trained MTANN suppressed ribs and clavicles in standard CXRs substantially, while the visibility of nodules and lung vessels was maintained. Here, we

developed a CADe scheme for detection of pulmonary nodules by use of the FFNN VDE technology to improve the sensitivity for nodules overlapping ribs and clavicles and to reduce FPs.

B. FFNN SCHEME FOR THE LUNG NODULE DETECTION

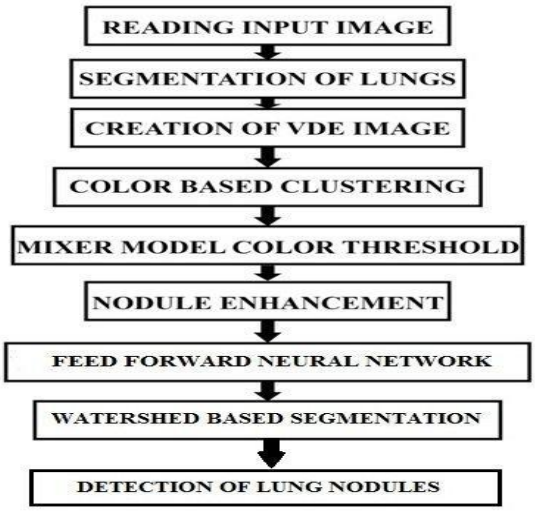

Fig.1. Block Diagram of FFNN Technique

SEGMENTATION OF LUNGS

To improve the performance of the CAD in Medical field, there are many researches are conducted. To provide a reliable and accurate detection of nodules in the CXR images, the segmentation of lungs is the most needed pre processing step in different types of CAD. The Lung Segmentation is very important to find out the lung nodules which present in border and edge portions of the lung. The small nodules in the lung are missed by seeing through naked eyes. Thus, the proposed algorithm is used to improve the sensitivity of the lung nodule image.

Techniques employed in segmentation are Thresholding, Deformable model based segmentation, Shape model and Edge model. Threshold-based segmentation approach consisting of four steps: (i) the large airway from the lung region was removed by isotropic diffusion method applied to smooth edges followed by region growing. ii) to remove the pulmonary vessels the optimal thresholding was finding. (iii) the largest threshold is applied to detect the anterior and posterior junctions to spate the left and right lungs and (iv) morphological smoothing is applied at the lung boundary along the mediastinum and lung wall based on the structure of the airway tree.

Lung segmentation techniques of the second category use deformable boundary models, such as active contours (snakes), *level sets* (LS). This model started from an initial segmentation obtained by a threshold estimated from CXR data. It is used to classify abnormal areas within each lung field. Silveira et al used a 2D geometric LS active contour being initialized at the boundary of the chest region, which was then automatically split into two regions representing the left and right lungs.

To improve the segmentation accuracy, shape-based techniques add prior information about the lung shape to image signals. First the ASM matching method is used to get a rough initial segmentation of the lung borders. Second, a global optimal surface finding method is used to find a refined smoothed segmentation of the lungs. The edge-model-based lung segmentation is performed using spatial edge-detector filters or wavelet transforms. The various Edge points i.e., themediastinal, costal, top, and bottom edge points were detected by spatial edge-detector filters and combined to define a closed contour for the lung borders.

VIRTUAL DUAL ENERGY RADIOGRAPHY

To utilize the differing physical properties of soft-tissue and bony structures that affect the attenuation of x-ray neurons at different x-ray energies, the dual energy imaging is used. It uses a dedicated hardware to capture a low energy image and high energy image during a single examination. For energy subtraction, the bone or soft tissue region get masked for the interpretation. The rib and soft tissue components of the CXRs get separated by means of Virtual Dual Energy Radiography technique. The benefits of applying this VDE Radiography are:

- There is no additional radiation dose is required for the patients.
- There is no need of any specialized equipment for the generation of the VDE images.

In our CADe scheme, we applied the VDE technology to reduce the rib induced False Positives and to find the nodules which are overlapping with the ribs and clavicles in the lungs. This VDE technology performs by two stage Enhancement technique ie. by watershed based segmentation and by grey level morphology.

GRAY LEVEL CO-OCCURRENCE MATRIX (GLCM)

To analyze the texture of 2D image, the GLCM is widely used. This GLCM matrix stores the co occurrence frequencies of the pairs of grey levels which are grouped by a distance and orientation. For the 2D method, it exploits eight directions in a single 2D plane. Then from the constructed GLSM, we extract eight features including energy, entropy, correlation, inverse differential moment, inertia, cluster shade, cluster prominence and Haralick correlation. The features are

Area: It gives the actual number of pixels in the ROI.

Convex Area: It gives the number of pixels in convex image of the ROI.

Equivalent Diameter: It is the diameter of a circle with the same area as the ROI.

$$\text{Equivalent Diameter} = \frac{\sqrt{4*AREA}}{\sqrt{\pi}}$$

Solidity: It is the proportion of the pixels in the convex hull that are also in the ROI.

$$\text{Solidity} = \frac{SOLIDITY}{CONVEX\ AREA}$$

Energy: It is the summation of squared elements in the GLCM and its value ranges between 0 and 1.

$$\text{Energy} = \sum_{k=0}^{n} p^2(i,j)$$

Contrast: It is the measure of contrast between an intensity of pixel and its neighbouring pixels over the whole ROI, where N is the number of different gray levels.

$$\text{Contrast} = \sum_{i}^{N} \sum_{j}^{N} (i-j)^2 p(i,j)$$

Homogeneity: It is the measure of closeness of the distribution of elements in the GLCM to the GLCM of each ROI and its value ranges between 0 and 1.

$$\text{Homogeneity} = \sum_{i,j} \frac{p(i,j)}{1+|i-j|}$$

Correlation: It is the measure correlation of pixel to its neighbor over the ROI.

$$\text{Correlation} = \sum_{i}^{N} \sum_{j}^{N} \frac{p(i,j) - \mu_r \mu_c}{\sigma_r \sigma_c}$$

Eccentricity: The eccentricity is the ratio of the distance between the foci of the ellipse and its major axis length.

 ISSN: 2321-7782 (Online) ISSN: 2347-1778 (Print)

NODULE ENHANCEMENT

For the detection of nodules here we are using two stage nodular enhancements with the help of SVM classifier to improve the sensitivity of the nodule detection and also to decrease the FP rate. In the first stage, grey level morphological operation was induced for the detection of the nodules overlapping ribs and clavicles.

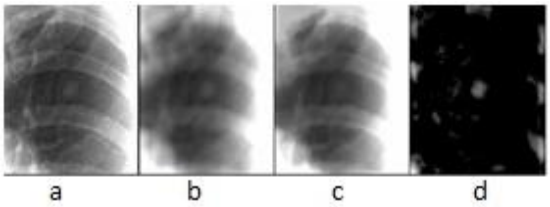

Fig: 2. Nodule enhancement by using the gray-level morphologic filter. (a) ROI with a nodule. (b) Enhancement of the nodule by using the gray-level morphologic filter with the nodule Gaussian template. (c) Enhancement of ribs by using the gray-level morphologic filter with the rib line templates (d) Nodule enhanced by subtracting (c) from (b).

In the second stage, the watershed segmentation was processed to detect the lung nodules accurately. Features are extracted from these segmented candidates for effectively determining the feature space, including one of the new features based on the edge detector to eliminate one of the major FP sources, rib crossings. Finally, the Gaussian kernel filter classifies the nodule candidates as nodules or non-nodules accurately.

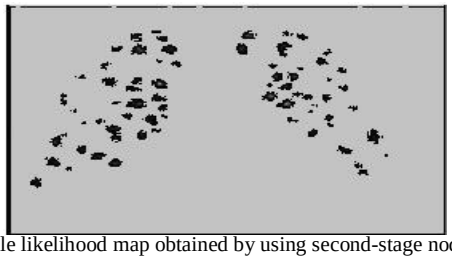

FIG.3. Nodule likelihood map obtained by using second-stage nodule enhancement.

FEED FORWARD NEURAL NETWORK

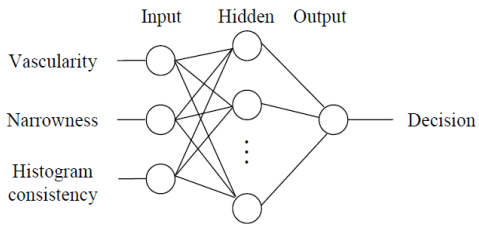

Fig.4. Basic Block Diagram of FFNN

Feed-forward ANN allow signals to travel one way only; from input to output. There is no feedback (loops) i.e. the output of any layer does not affect that same layer. Feed-forward ANNs tend to be straight forward networks that associate inputs with outputs. They are extensively used in pattern recognition. This type of organization is also referred to as bottom-up or top-down. The behaviour of a Feed Forward ANN (Artificial Neural Network) depends on both the weights and the input-output function (transfer function) that is specified for the units. This function typically falls into one of three categories:

- Linear (or ramp),
- Threshold,
- Sigmoid.

For **Linear units**, the output activity is proportional to the total weighted output.

For **Threshold units**, the output is set at one of two levels, depending on whether the total input is greater than or less than some threshold value. The total input I is given by the formula

$$I = \sum_{i=0}^{n} WiXi$$

where X1, X2, X3… Xn are the n Inputs to the Artificial Neuron and W1, W2, W3 … Wi are the weights associated to these input links.

For **sigmoid units**, the output varies continuously but not linearly as the input changes. This unit calculates the activity Xi using the function of total weighted input and this is called activation function used in the sigmoid unit and it is defined as:

$$\text{Sigmoid (Xi)} = \frac{1}{1+e^{-x}}$$

Where x is the sum of total weighted inputs to the particular node and e=2.732

WATERSHED SEGMENTATION

To refine the rough segmentation provided by morphologic filtering, we developed a clustering watershed segmentation technique. Peaks within the rough nodule candidate region in the nodule-enhanced image were obtained and used for initializing the watershed segmentation algorithm. For the application of watershed segmentation, the gray scale of the ROI was first inverted so that the peaks became local minima. With the watershed segmentation the rough nodule candidate region was divided into several catchment basins. Each minimum point was surrounded by a catchment basin associated with it; thus, there were one or more peaks, each of which was surrounded by a cluster of connected pixels that constituted a catchment basin.

From the multiple catchment basins, a single nodule candidate region was determined by using the following clustering method: First, a primary cluster was defined as a cluster that contained the nodule candidate location as a point determined by the initial nodule candidate detection step. Next, clusters connected to the primary cluster were added. The connected clusters were identified by using the criterion that the minimum value between the peak in the primary cluster and each of the other peaks was larger than a threshold value. The fig illustrates a segmented nodule candidate obtained by using the clustering watershed segmentation.

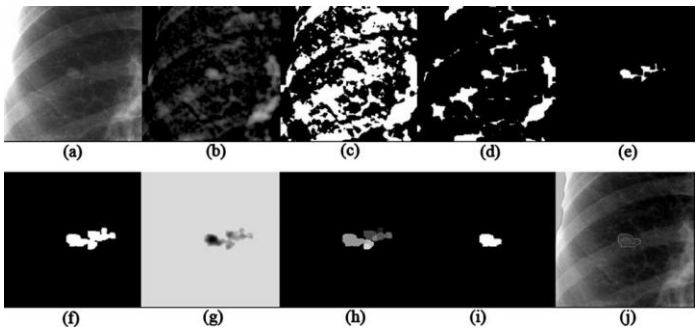

FIG.5.Nodule candidate segmentation by using our clustering watershed segmentation method. (a) ROI with a nodule. (b) First-stage nodule enhancement image by using background-trend correction and a gray-level morphologic filter. (c) Regions obtained by thresholding of the image (b) with a low positive threshold value. (d) Regions after erosion. (e) Connected region representing a rough nodule candidate. (f) Candidate region after dilation.(g) Inverted image. (h) Result with watershed segmentation alone. One region was divided into multiple small segments catchment basins. (i) Nodule candidate segmented by our clustering watershed segmentation. (j) Nodule contour.

III. CONCLUSION

The method is aimed at the development of a model to an efficient method for development of computerized scheme for detection of lung nodules by incorporating VDE image in which ribs and clavicles were suppressed by FFNN technique. The performance of the CAD scheme (87% sensitivity with 5 FPs/image) provided a substantial improvement against the original CAD scheme (78% sensitivity with 5 FPs/image).

References

1. C. I. Henschke, D. I. McCauley, D. F. Yankelevitz, D. P. Naidich, G. McGuinness, O. S. Miettinen, D. M. Libby, M. W. Pasmantier, J. Koizumi, N. K.Altorki, and J. P. Smith, "Early lung cancer action project: Overall design and findings from baseline screening," Lancet, vol. 354, pp. 99–105, Jul. 10, 1999.
2. H. Zhao, S. C. Lo, M. Freedman, and Y. Wang, "Enhanced lung cancer detection in temporal subtraction chest radiography using directional edge filtering techniques," presented at the Proc. SPIEMed. Imag. Image Process. San Diego, CA, 2002.
3. P. K. Shah, J. H. Austin, C. S. White, P. Patel, L. Haramati,G. D. Pearson, M. C. Shiau, and Y. M. Berkmen, "Missed non-small cell lung cancer: Radiographic findings of potentially resectable lesions evident only in retrospect," Radiology, vol. 226, pp. 235–241, Jan. 2003.
4. F.Li, R. Engelmann, K. Doi, and H. MacMahon, "Improved detection of small lung cancers with dual-energy subtraction chest radiography," AJR Amer. J Roentgenol., vol. 190, pp. 886–891, Apr. 2008.
5. B.Van Ginneken, B. M. ter Haar Romeny, and M.A.Viergever, "Computer-aided diagnosis in chest radiography: A survey," IEEE Trans. Med. Imag., vol. 20, no. 12, pp. 1228–1241, Dec. 2001.
6. K.Suzuki, J.Shiraishi, H.Abe, H.MacMahon, and K.Doi, "False-positive reduction in computer-aided diagnostic scheme for detecting nodules in chest radiographs by means of massive training artificial neural network," Acad. Radiol., vol. 12, pp. 191– 201, Feb. 2005.
7. R. C. Hardie, S. K. Rogers, T.Wilson, and A. Rogers, "Performance analysis of a new computer aided detection system for identifying lung nodules on chest radiographs," Med. Image Anal., vol. 12, pp. 240–258, Jun. 2008.
8. T. F. Cootes, A. Hill, C. J. Taylor, and J. Haslam, "Use of active shape models for locating structures in medical images," Image Vis. Comput.,vol. 12, pp. 355–365, 1994.
9. L. Vincent and P. Soille, "Watersheds in digital spaces: An efficient algorithm based on immersion simulations," IEEE Trans. Pattern Anal. Mach.Intell., vol. 13, no. 6, pp. 583–598, Jun. 1991.
10. J.Wei, Y. Hagihara, A. Shimizu, and H. Kobatake, "Optimal image feature set for detecting lung nodules on chest X-ray images," in Proc. Comput.-Assisted Radiol. Surg., 2002, pp. 706–711.
11. J. Shiraishi, Q. Li, K. Suzuki, R. Engelmann, K. Doi, "Computer-aided diagnostic scheme for the detection of lung nodules on chest radiographs: Localized search method based on anatomical classification," Med. Phys., vol. 33, pp. 2642– 2653, Jul. 2006
12. R. M. Nishikawa, M. L. Giger, K. Doi, C. E. Metz, F. F. Yin, C. J. Vyborny, and R. A. Schmidt, "Effect of case selection on the performance of computer-aided detection schemes," Med. Phys., vol. 21, pp. 265–269, Feb. 1994.
13. Sheng Chen and Kenji Suzuki, Member, IEEE "Computerized Detection of lung nodules by means of "Virtual Dual-Energy" Radiography" IEEE Transactions on Biomedical Engineering, vol. 60, no. 2, February 2013.

